Exploring the use of displaced-beam scintillometer for daytime measurement of surface energy fluxes over a Mediterranean Olive Orchard

Article *in* Italian Journal of Agrometeorology · August 2014

CITATION
1

READS
178

8 authors, including:

Carmelo Cammalleri
European Commission
74 PUBLICATIONS **2,689** CITATIONS
SEE PROFILE

Carmelo Agnese
Università degli Studi di Palermo
54 PUBLICATIONS **824** CITATIONS
SEE PROFILE

Joseph Alfieri
United States Department of Agriculture
139 PUBLICATIONS **4,143** CITATIONS
SEE PROFILE

Teodoro Georgiadis
Italian National Research Council
259 PUBLICATIONS **1,825** CITATIONS
SEE PROFILE

Exploring the use of displaced-beam scintillometer for daytime measurement of surface energy fluxes over a Mediterranean Olive Orchard

Carmelo Cammalleri[1,], Carmelo Agnese[2], Joseph G. Alfieri[3], Antonino Drago[4], Teodoro Georgiadis[5], Antonio Motisi[6], Maurizio Sciortino[7], Henk A.R. de Bruin[8]*

Abstract: *Studies have shown that the footprint of a single eddy covariance (EC) system may not yield representative measurements of the turbulent fluxes at the field scale for sparse vegetated surfaces, whereas scintillometry, due to its larger footprint, may be more suitable for this purpose. However, the latter approach strongly relies on the Monin-Obukhov similarity theory (MOST) that strictly applies in the inertial sub-layer only. This work aims at experimentally confirm the reliability of displaced-beam laser scintillometer (DBLS) measurements over an olive orchard against two EC systems during summer and autumn months of 2007 through 2009. It was found that the DBLS underestimated both the momentum and sensible heat fluxes by 15 to 20% when established retrieval procedures were applied. A new method to determine the sensible heat flux from the DBLS based on the addition of a single-height wind speed measurement was tested, yielding estimates that compare well with the EC observations, with discrepancies in sensible heat fluxes of about 30 to 40 W m^{-2}.*
Keywords: *evapotranspiration, micrometeorological measurements, sparse tall crops,* Olea europaea.

Riassunto: *Studi hanno dimostrato che le dimensione dell'impronta di un singolo sistema di correlazione turbolenta (EC) può non fornire misure rappresentative alla scala di campo nel caso di vegetazione sparsa, mentre la scintillometria, grazie alla sua maggiore impronta, potrebbe essere più adatta a questo scopo. Tuttavia, quest'ultimo approccio si basa sulla teoria di similitudine atmosferica di Monin-Obukhov (MOST) che è strettamente valida solo nel sub-strato inerziale. Obiettivo di questo lavoro è la conferma sperimentale dell'affidabilità delle misure di uno scintillometro laser a doppio fascio (DBLS) in corrispondenza di un oliveto, mediante il confronto con le misure acquisite da due sistemi EC durante i mesi estivi e autunnali dal 2007 al 2009. I risultati mostrano che il DBLS sottostima i flussi di calore sensibile e quantità di moto del 15-20% quando vengono adottate le classiche procedure di calcolo. È stato quindi testato un nuovo metodo di stima dei flussi di calore sensibile basato sull'aggiunta di una misura della velocità del vento ad un singola altezza, ottenendo stime in migliore accordo con le misure EC, con differenze nell'ordine di 30 -40 W m^{-2}.*
Parole chiave: *evapotraspirazione, misure micrometeorologiche, piante alte sparse,* Olea europaea.

1. INTRODUCTION

In Mediterranean regions the growing season is usually very dry, which leads to significant crop water stress. As a result, it is often necessary to irrigate crops in this region in order to maximize crop yield and productivity. This, in conjunction with the reduced water availability during the last 20 years (UNEP/MAP-PlanBleu, 2009), underscores the need for accurate information regarding crop water uses in order to optimize water resource management. Although remote sensing-based energy balance models are a cost effective method for mapping evapotranspiration over large areas (Schmugge *et al.*, 2002) and have been utilized in numerous environments (*e.g.*, Cammalleri *et al.*, 2012; Choi *et al.*, 2009; French *et al.*, 2005; Timmermans *et al.*, 2007), in-situ observations are essential for investigating land-atmosphere exchange processing and validating both numerical and remote sensing-based models.

Although the eddy covariance (EC) technique is well suited to measure turbulent fluxes over short dense vegetation, scintillometry may be more appropriate for collecting flux data over tall sparse canopies (Vogt *et al.*, 2004). This is because scintillometry typically

*Corresponding author: cammillino@gmail.com
[1] Post-doc Researcher, Department of Civil, Environmental, Aerospace, Materials Engineering (DICAM), Università degli Studi di Palermo, Palermo, Italy.
[2] Full Professor (retired), Department of Agricultural and Forest Sciences (SAF), Università degli Studi di Palermo, Palermo, Italy.
[3] Associate Researcher, U.S. Department of Agriculture, Agricultural Research Service, Hydrology and Remote Sensing Laboratory, Beltsville, 20705-2350 MD, USA.
[4] Researcher, Assessorato Risorse Agricole e Alimentari, Regione Siciliana, Palermo, Italy.
[5] Researcher, Istituto di Biometeorologia (IBIMET) - CNR, Bologna, Italy.
[6] Full Professor, Department of Agricultural and Forest Sciences (SAF), Università degli Studi di Palermo, Palermo, Italy.
[7] Researcher, Agenzia per le Nuove Tecnologie, l'Energia e lo Sviluppo Economico Sostenibile (ENEA), C.R. Casaccia, Rome, Italy.
[8] Professor Emeritus, Wageningen University, freelance consultant Bilthoven, The Netherlands.
Received 24 September 2013, accepted 21 March 2014.

samples a larger footprint compared to EC under the same conditions of fetch and sensor height due to the wider shape of its source area (Hoedjes *et al.*, 2007). Scintillometry also offers other potential advantages over EC: not only it can provide reliable data for short (<< 30 min) measurement periods, but it can also collect these data quite near the surface (Thiermann and Grassl, 1992).

Scintillometry, however, relies on experimentally-derived universal functions underpinned by Monin-Obukhov Similarity Theory (MOST) to link the transport of scalar quantities to turbulent properties. Since MOST is strictly valid only within the surface boundary layer (SBL), the lowest part of atmospheric boundary layer where fluxes do not change significantly with height (Stull, 1988), the universal function are, in a strict sense, only applicable to the SBL. Because the basic assumptions of MOST do not hold in the roughness sublayer (RL), the region of the SBL extending from the surface to the blending height (z^*) where the influence of individual roughness elements is still evident (Raupach *et al.*, 1991), the universal function used by scintillometry may not be valid. As pointed out by Raupach *et al.* (1996), because MOST does not consider many of the mechanisms of turbulent production, such as the development of coherent eddies, that occur within the RL, measurement techniques based on MOST tend to underestimate the turbulent fluxes within the RL.

In contrast to short dense canopies, where the thickness of the RL is most often negligible, z^* can be significant over tall sparse canopies (de Ridder, 2010). In order to extend the applicability of MOST-based measurement to the RL, some authors (*e.g.*, Chen *et al.*, 1997; Odhiambo and Savage, 2009a) have suggested using the height of the sensor above the ground level as the length scale, instead of the height above zero-plane displacement. Alternatively, Cellier and Brunet (1992) suggested adjusting both wind speed and temperature profiles by introducing empirically-determined multiplicative factors to account for the enhanced turbulence within the RL (Graefe, 2004; Mölder *et al.*, 1999).

The main objective of this study is to investigate the utility of displaced-beam laser scintillometer (DBLS) over tall sparse vegetation for determining the daytime turbulent fluxes by comparing measurements from DBLS with EC measurements collected in the same study site. Additionally, an alternative method for processing DBLS data was explored. This method, which utilizes additional measurements of horizontal wind speed, should be less sensitive to the uncertainties linked to the sensor set-up and configuration; and therefore, it should provide turbulent flux measurements that better agree with EC measurements without the need for empirical corrections.

2. THEORETICAL BACKGROUND

Actual evapotranspiration is often derived as the residual of the simplified surface energy balance equation as applies to the soil-plant-atmosphere system,

$$R_n - G_0 = H + \lambda ET \quad (1)$$

where R_n (W m^{-2}) is the net radiation, G_0 (W m^{-2}) is the soil heat flux at the surface, H (W m^{-2}) is the sensible heat flux and λET (W m^{-2}) is the latent heat flux. The main challenge of this approach is the acquisition of reliable turbulent fluxes. Among the numerous techniques developed to partition the available energy, $R_n - G_0$, into H and λET, those compared in this study, EC and DBLS, are described below.

2.1 Eddy Covariance

The eddy covariance technique is a well-established approach based on the direct measurement of turbulent transport. As described in the literature (*e.g.*, Kaimal and Finnigan, 1994; Stull, 1988; Rosenberg *et al.*, 1983), the vertical flux of a generic scalar can be computed as the covariance between the vertical wind velocity and the scalar density. Following this definition, it is possible to derive the mechanical shear production, and then the momentum flux in terms of the friction velocity (u_*, m s^{-1}) as:

$$u_* = \left(\overline{u'w'}^2 + \overline{v'w'}^2\right)^{0.25} \quad (2)$$

where $\overline{u'w'}$ is the covariance between the horizontal wind velocity component in the streamwise direction (u, m s^{-1}), and the vertical wind velocity (w, m s^{-1}) and $\overline{u'w'}$ is the covariance between the horizontal crosswind component (v, m s^{-1}) and w. Similarly, H can be defined as:

$$H = \rho c_p \overline{w'T'} \quad (3)$$

where ρ (kg m^{-3}) is the air density, c_p (J kg^{-1} K^{-1}) is the specific heat capacity of air at a constant pressure and $\overline{w'T'}$ is the covariance between temperature (T, K) and w. Finally, the vertical flux of water vapor expressed in terms of energy, *i.e.*, λET, can be defined as:

$$\lambda ET = \lambda \overline{w'q'} \quad (4)$$

where λ (J kg^{-1}) is the latent heat of vaporization and $\overline{w'q'}$ is the covariance between the water vapor density (q, kg m^{-3}) and w. The covariances required by Eqs.

(2) - (4) are derived from the high frequency EC data after applying numerous post-processing corrections that are described briefly in the data collection section.

2.2 Displaced-Beam Laser Scintillometer

Scintillometry takes advantage of the relationship between variations in light intensity due to fluctuations in the refractive index of air (n), which are known as scintillations, and turbulent intensity to measure the transport of sensible heat. More specifically, DBLS is designed to measure the structure parameter of the refractive index of air, (C_n^2, $m^{-2/3}$) and the dissipation rate of turbulent kinetic energy (ε, $m^2 s^{-3}$) from which both H and u_* can be determined (Thiermann, 1992). This type of scintillometer operates in the red portion of the spectrum (λ_s = 670 nm) and consists of a transmitter that produces a laser signal that is split into two beams of orthogonal polarization and a receiver that measures the fluctuations in the signal intensity. The variance of the amplitude of both beams, namely B_{11} and B_{22}, as well as the covariance (B_{12}) can be expressed as:

$$B_{12} = 0.124 C_n^2 K^{7/6} R^{11/6} f_B\left(\frac{l_0}{\sqrt{\lambda_s R}}, \frac{d}{\sqrt{\lambda_s R}}, \frac{D}{\sqrt{\lambda_s R}}\right) \quad (5)$$

where K is the optical wave number ($= 2\pi/\lambda_s$), R is the propagation path length (m) and f_B is a function of the three dimensionless quantities characterizing the inner length scale (l_0, m), the separation between the two beams (d , m) and the aperture width of the two detectors (D, m) (Thiermann (1992). B_{11} and B_{22} can be expressed in a similar fashion by assuming d equal to zero. For a given combination of d and D, l_0 can be estimated directly from the ratio

$$r_{12} = \frac{B_{12}}{\left(B_{11} B_{22}\right)^{1/2}}$$

which allows C_n^2 to be derived by rearranging Eq. (5) (Thiermann, 1992).

As discussed by Wesely (1976) and Moene (2003), when humidity levels are low, humidity effects can normally be ignored so that the structure parameter for temperature (C_T^2, $K^2\ m^{-2/3}$), can be obtained directly from C_n^2 as:

$$C_T^2 = \left(\frac{T^2}{bP}\right)^2 C_n^2 \quad (6)$$

where P (kPa) is the atmospheric pressure and b (0.789×10^{-3} K kPa^{-1}) is the scaling coefficient for the refractive index of air at 670 nm.

Following Hill (1997), the dissipation rate of the kinetic energy of the turbulence ε can be estimated from l_0 according to:

$$\varepsilon = \nu^3 \left(\frac{7.4}{l_0}\right)^4 \quad (7)$$

where ν ($m^2 s^{-1}$) is the kinematic viscosity of air.

2.2.1 Estimating H and u_* using MOST

The standard approach for determining the turbulent fluxes from scintillometric data (referred to as SBL-MOST hereafter) is based on the assumptions of MOST. According to MOST, ε and C_T^2 can be both expressed in dimensionless form by scaling them by u_* and the temperature scale, T_* (K), respectively:

$$\frac{k(z-d_0)\varepsilon}{u_*^3} = f_\varepsilon\left(\frac{z-d_0}{L}\right) \quad (8a)$$

$$\frac{C_T^2 (z-d_0)^{2/3}}{T_*^2} = f_T\left(\frac{z-d_0}{L}\right) \quad (8b)$$

where k is the von Kármán constant (0.41), z (m) the measurement height , d_0 (m) the zero-plane displacement height, L (m) the Obukhov length, and f_ε and f_T the universal functions of $\left(\frac{z-d_0}{L}\right)$.

The temperature scale can be defined as:

$$T_* = \frac{H}{\rho c_p u_*} = \frac{\overline{w'T'}}{u_*} \quad (9)$$

while L can be defined as:

$$L = -\frac{\rho c_p T u_*^3}{kgH} \quad (10)$$

The zero-plane displacement height is commonly taken to be two-thirds of the canopy height following Brutsaert (1982).

The universal functions f_ε and f_T have to be determined experimentally and, unfortunately, there is no consensus regarding the appropriate mathematical forms (for a detailed discussion, see the recent review by Savage, 2008). In this study, we adopted the functions proposed by Hartogensis (2006) and de Bruin *et al.* (1993). For unstable conditions (<0) these are expressed as:

$$f_\varepsilon\left(\frac{z-d_0}{L}\right) = \left(1 - 15.1\frac{z-d_0}{L}\right)^{-1/3} - \frac{z-d_0}{L} - 0.16 \quad (11a)$$

$$f_T\left(\frac{z-d_0}{L}\right)=4.9\left(1-9\frac{z-d_0}{L}\right) \quad (11b)$$

Using these relationships, T_* and u_* can be determined by an iterative procedure and H can be determined by rearranging Eq. (9).

2.2.2 Alternative approach in the RL

The proposed alternative procedure aims at yielding reliable estimates of H when DBLS is installed within the RL. The main requirement of this methodology is the addition of a low-frequency horizontal wind speed measurement above the canopy (U, m s^{-1}) to determine u_*, whereas T_* is directly derived from scintillometer measurements by taking into account the effects of l_0 on the relationship between B_{11} (or B_{22}) and C_n^2 by means of the Hill and Clifford (1978) spectrum. Specifically, the estimation of u_* is obtained by inverting the definition of wind speed profile as:

$$u_*=\frac{kU}{\ln\left(\frac{z-d_0}{z_{0m}}\right)-\Psi_m\left(\frac{z-d_0}{L}\right)} \quad (12)$$

where Ψ_m is the atmospheric stability correction function defined by Paulson (1970) and Webb (1970), and z_{0m} (m) is the roughness length for momentum, which is assumed equal to one-ninth of the canopy height. For the first iteration step Ψ_m is assumed equal to zero.

This estimate of u_* can be used to invert Eqs. (7) and (8a), assuming L = 0, to obtain an l_0 that is in agreement with the new estimate of u_*:

$$l_0=\frac{7.4\nu^{3/4}}{u_*^{3/4}}\left[\frac{k(z-d_0)}{f_\varepsilon\left(\frac{z-d_0}{L}\right)}\right]^{1/4} \quad (13)$$

The value of l_0 obtained from Eq. (13) can be used to derive the spectral function (f_B) by means of an empirical fitting of Hill and Clifford (1978) spectrum:

$$f_B=b\frac{a^2}{(l_0-l_{0c})^2+a^2} \quad (14)$$

where a, b and l_{0c} are fitting parameters obtained using characteristics of the scintillometer (D, λ_s) and path length (R). Equation (14) was fitted assuming d equal to zero, thereby linking f_B to B_{11} (or B_{22}). A simple fit is used in lieu of the effective spectrum to reduce the computational complexity of the subsequent analysis; however it is substantially analogous to directly solve the full spectrum for the known instrument configuration.

The scintillometer-measured value of B_{11} (or B_{22}) can be used with f_B to derive a new estimation of C_n^2 from Eq. (5), hence T_* is obtained using Eqs. (6), (8b) and (11b) assuming again L = 0. Once both u_* and T_* are known, H can be obtained through Eq. (9), as well as L via Eq. (10). The procedure, starting from Eq. (12), has to be iterated (using the L value obtained at the previous step) until convergence is achieved.

3. STUDY AREA AND MATERIALS

3.1 Site Description

The experiments were carried out during the growing seasons (approximately June through October) of 2007 to 2009 at the "*Rocchetta*" olive farm (Fig. 1), located in southwestern Sicily (Italy) approximately 5 km from Castelvetrano (TP) town (37°38'35" N, 12°50'50" E). As highlighted by Fig. 1, the landscape is generally flat and highly fragmented, with small fields – typically the fields are only a few hectares in size - containing a variety of different crop types. The soil is rather homogeneous, and can be classified as silty clay loam following the USDA classification, with mean clay, silt and sand contents of about 24, 16 and 60%, respectively. The region has a typical Mediterranean climate characterized by high temperatures and low rainfall during the summer months (June through September) and moderate rainfall during autumn and winter (October to April). The annual rainfall during the period from 2005 to 2010 ranged from 450 to 650 mm while the evaporative demand during the same period ranged between 1000 and 1200 mm.

Specifically, the experiment was conducted in a 13 ha orchard (Fig. 1) where *cv. "Nocellara del Belice"* olive trees were grown. The trees are distributed following a regular grid of about 8 × 5 m^2 and the mean canopy height was approximately 3.7 m in 2007 and 3.3 m in both 2008 and 2009. This variation was due to pruning of the canopy performed during the winter of 2007. The orchard is mainly irrigated by means of a drip irrigation system.

3.2 Data Collection[1]

Two EC systems were used during the experiments. The first system (referred to EC1 hereafter) is part of the CarboItaly network (Papale, 2006) and is located in the northern part of the experimental

[1] Trade and company names are given solely for the purpose of providing specific information and do not imply recommendation or endorsement by the authors.

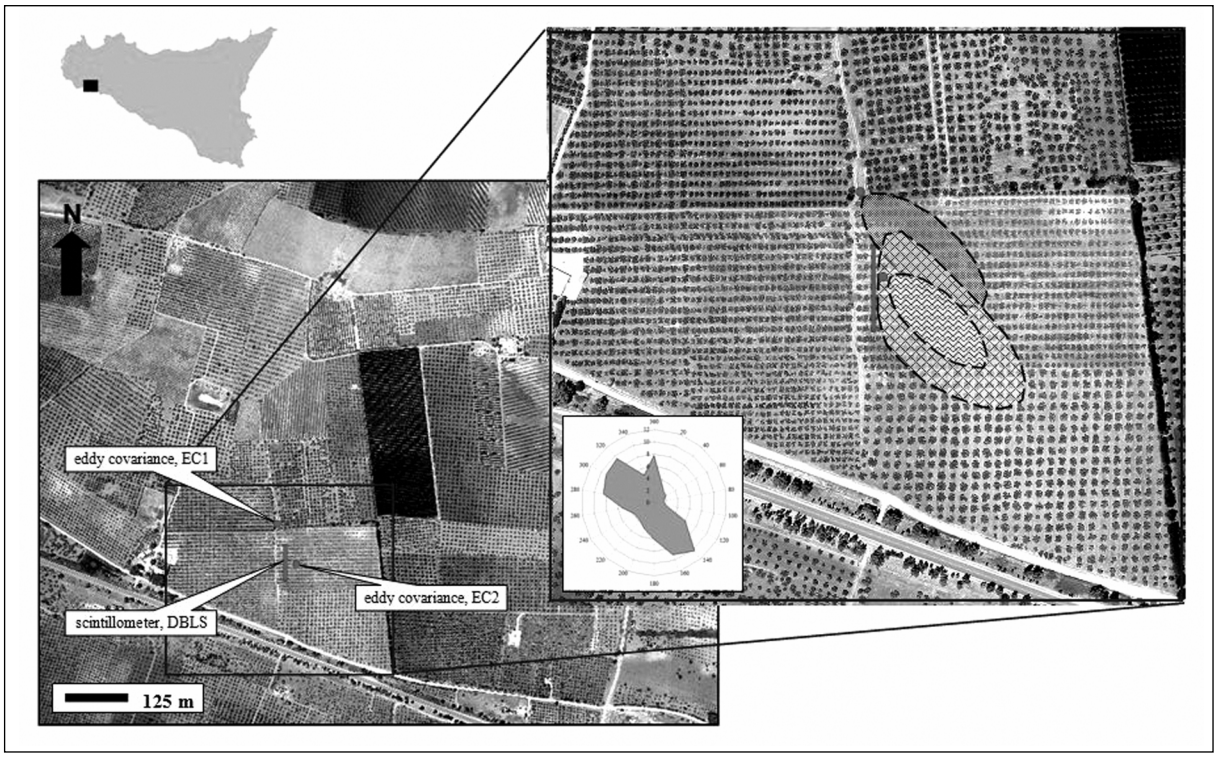

Fig. 1 - An orthophoto of the study area acquired during an airborne overpass on 11 June 2008 with a Canon EOS 20D digital camera with a spatial resolution of 0.4 m is shown. The location of the two eddy covariance (EC1 and EC2) and displaced-beam laser scintillometer (DBLS) installations are also reported. The inset highlights the monitored olive orchard with the filled areas representing the measurement footprints for the predominant daytime condition (L = -50 m, u = 3.1 m s^{-1} and direction 140°). A wind rose shows the distribution of wind direction during daytime hours only.
Fig. 1 - Ortofoto dell'area di studio acquisita con volo aereo in data 11 giugno 2011 mediante camera digitale EOS 20D alla risoluzione spaziale di 0.4 m. Vengono riportate le posizioni delle due stazioni di flusso turbolento (EC1 e EC2) e dello scintillometro laser (DBLS). Il dettaglio mostra l'oliveto monitorato e le impronte dei tre strumenti durante le condizioni giornaliere predominati (L = -50 m, u = 3.1 m s^{-1} in direzione 140°). La rosa dei venti mostra la distribuzione di frequenza della direzione del vento durante le sole ore diurne.

field (Fig. 1). This system consisted of a net radiometer (NR-Lite-L, Kipp & Zonen, The Netherlands) deployed at an height of 8.5 m, a three-dimensional sonic anemometer (CSAT3-3D, Campbell Scientific Inc., Logan, Utah, USA) and an open-path infrared gas analyzer (LI7500, Li-Cor Biosciences Inc., Lincoln, Nebraska, USA) co-located at a height of 8 m, and three self-calibrating flux plates (HFP01SC, Hukseflux, The Netherlands) installed at a depth of 0.05 m below the canopy, in the plant interspace, and within the interrow space, respectively. Additional instruments include a thermo-hygrometer and a cup anemometer. In particular, the cup anemometer (A100L2, Vector Instruments, Rhyl, UK) was installed at the same height of sonic anemometer.

The high frequency measurements were collected at a sampling rate of 10 Hz and stored on a datalogger (CR3000, Campbell Scientific) equipped with a PCMCIA memory card. The measurements from the slow response sensors were stored on the datalogger as half-hourly means. Data post-processing was conducted following the Fluxnet standard protocol (Aubinet *et al.*, 2000); the main steps include a coordinate rotation to align the measurement coordinate system with the mean streamwise flow, a correction for spectral attenuation, and the adjustment for buoyancy and water vapor effects (Webb *et al.*, 1980; Moncrieff *et al.*, 1997).

The second EC system (referred to as EC2 hereafter) was installed in 2009 at the midpoint of the DBLS path (Fig. 1). This system consisted of a four component net radiometer (CNR-1, Kipp & Zonen) mounted at a height of 8.5 m, a three-dimensional sonic anemometer (CSAT3-3D, Campbell Scientific Inc., Logan, Utah, USA) and an open-path infrared gas analyzer (LI7500, Li-Cor Biosciences Inc., Lincoln, Nebraska, USA) co-located at a height of 7 m, and a pair of self-calibrating heat flux plates (HFP01SC,

Hukseflux) installed at a depth 0.1 m (one below the plant canopy and one in the interrow space). The sampling rate for the fast response sensors in this system was 20 Hz. Also for this system a cup anemometer (A100L2, Vector Instruments, Rhyl, UK) was installed at the same height of sonic anemometer. The slow response measurements were stored as half-hourly means. All of the data were recorded on a datalogger (CR5000, Campbell Scientific) equipped with a PCMCIA memory card. The high frequency data were post-processed adopting the procedure implemented by Manca (2003) which is substantially analogous to the Fluxnet standard protocol.

The DBLS, which was installed in the middle of the experimental site (Fig. 1), acquired data during three separate periods: July through September, 2007; August through October, 2008; and May through August, 2009. Specifically, the installation included a small aperture scintillometer (SLS20, Scintec AG, Germany) with an aperture size of 2.5 mm, beam displacement of 2.7 mm, beam divergence of 5 mrad, and operational wavelength of 670 nm. Both transmitter and receiver were installed on scaffolding iron frames separated by a path of approximately 96 m. The instrument height was 5.8 m for 2007 and 7.1 m for 2008 and 2009. The measurement path extended from north to south and was nearly perpendicular to the dominant daytime wind direction (see wind rose in Fig. 1).

Net radiation was measured using a two-component pyrradiometer (model 8111, Schenk GmbH - Germany), installed at a height of 8 m. The soil heat flux was computed from the measurements acquired by three self-calibrating heat flux plates (HFP01SC). All three plates were installed at a depth of 0.05 m, in a similar pattern as EC1. All data were acquired every two minutes using a signal-processing interface connected to a computer. The raw data from the scintillometer was the average of 20 acquisitions. Both H and λET were computed by the acquisition software; particularly, the latter is derived as a residual of the energy balance equation. Stability conditions, as well as the appropriate MOST relationships, were determined based on the direction of the air temperature gradient measured by a pair of aspirated temperature sensors (PT1000, Omega Engineering, Manchester, UK) positioned 4 and 6 m above ground level. During post-processing, the two-minute H flux estimates were aggregated to half-hour block averages to facilitate direct comparison with the EC measurements.

The energy balance closure was tested by means of the closure ratio (CR), which was computed as suggested by Prueger *et al.*, (2005) using only daytime (R_n > 100 W m^{-2}) data:

$$\mathrm{CR} = (R_n - G_0)/(H + \lambda ET) \tag{15}$$

Pernice *et al.* (2009) showed a satisfactory balance closure for EC1 (CR = 0.86); the closure for the EC2 system was equally satisfactory during the studied periods (CR = 0.90). However, because scintillometry estimates λET as the residual of the energy balance relationship, closure was forced for the EC systems by assigning all residual energy to λET in order to preserve the observed H. Additionally, in order to isolate the differences in turbulent fluxes, the R_n and G_0 data available from all the instruments were averaged and used as a common dataset of available energy for ECs and DBLS installations.

The footprints for EC1, EC2 and DBLS H fluxes were computed adopting the method proposed by Kormann and Meixner (2000) for modeling the analytical solution of the two-dimensional advection-diffusion equation for non-neutral stratifications. In the case of DBLS measurements, the along-path integration of single point footprints was performed adopting the weighting function suggested by Göckede *et al.* (2005). The footprints for the most frequent unstable daytime conditions (L = -50 m, u = 3.1 m s^{-1} and direction of 140°) are shown in the inset of Fig. 1. These footprints demonstrate that 90% of the measured fluxes were within the study field; it is also evident that the source area for installation EC2 is completely within the footprint of the DBLS.

3.3 Analysis Method

The differences between EC and DBLS were quantified by means of common statistical metrics, aiming at quantifying both the agreement and the correlation of the two datasets. Systematic differences were measured by means of the Mean Bias Difference (MBD):

$$\mathrm{MBD} = \frac{\sum_{i=1}^{n}(O_i - M_i)}{n} \tag{16}$$

where O_i and M_i are the EC and DBLS i-th observation, respectively, and n is the number of observations; whereas the overall (systematic and random) differences were measured using the Root Mean Square Difference (RMSD),

$$\mathrm{RMSD} = \sqrt{\frac{\sum_{i=1}^{n}(O_i - M_i)^2}{n}} \tag{17}$$

and the Mean Absolute Difference (MAD),

$$\mathrm{MAD} = \frac{\sum_{i=1}^{n} |O_i - M_i|}{n} \qquad (18)$$

In order to make comparable the results obtained for different years, the Relative Error (RE, %) was computed by dividing the MAD for the EC observed value. Additionally, the correlation between the two observed datasets was quantified by means of Pearson coefficient (r) of the linear regression, assuming the EC measurements as the independent variable. It was noticed that the intercept of the linear regression was almost negligible in all the cases; hence, we decided to force the regressions through the origin. This choice allows us to adopt the slope of the regression line as a synthetic descriptor of systematic errors.

4. RESULTS AND DISCUSSION

4.1 Analysis of the DBLS Data Processed Using Standard Stand-alone Method

The sensible heat flux measurements from the DBLS derived by using SBL-MOST were compared with the measurements collected by the EC systems in order to characterize the performance of the stand-alone DBLS technique. Since the main focus of the paper is the use of scintillometry for the assessment of evapotranspiration, the analysis was restricted to the unstable conditions that are typical in dry environments during daytime hours. Additionally, EC measurements are known to be less reliable during nighttime hours when turbulence is weak (Falge *et al.*, 2001), which is particularly true for sparse tall vegetations.

A comparison of the daytime flux measurements by the two methods shows a clear difference in the response of H to changing environmental conditions. As an example, the plots in Fig. 2 show R_n and H for two days: a typical clear-sky day (Fig. 2a-b) and a partly cloudy day (Fig. 2c-d), where it is evident that clouds passed over the site around 1130 GMT. Under clear-sky conditions, H measured via DBLS (Fig. 2a) varied smoothly over time while the corresponding measurements from EC1 (Fig. 2b) are noisier and more erratic. On the partly cloudy day, H measured using DBLS (Fig. 2c) shows an immediate and strong response to passing clouds

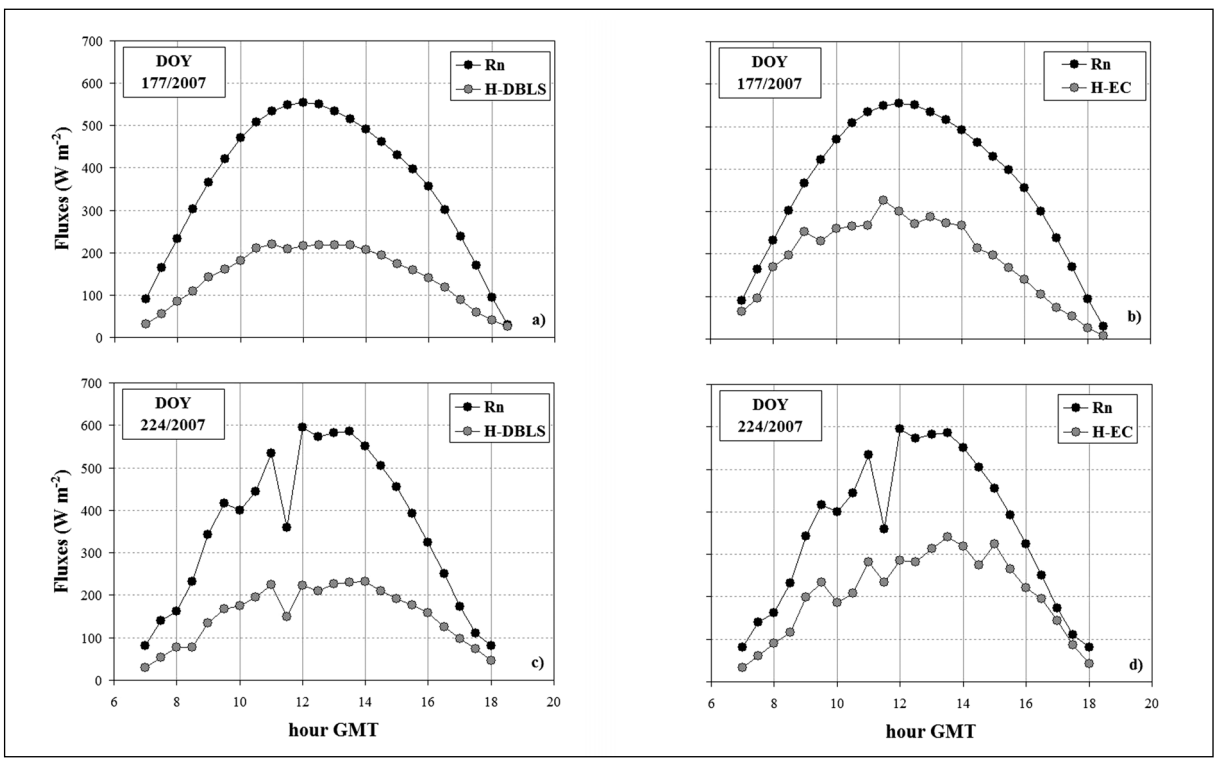

Fig. 2 - Daytime course of half-hour net radiation and sensible heat fluxes measured during a clear-sky (panels a and b) and a cloudy (panels c and d) day. Panels a) and c) show the DBLS measurements; panels b) and d) report the fluxes from EC1.
Fig. 2 - Andamento giornaliero della misure semi-orarie di radiazione netta e di flusso di calore sensibile durante un giorno limpido (pannelli a e b) ed uno parzialmente nuvolo (pannelli c e d). I pannelli a) e c) mostrano le misure acquisite dal sistema DBLS mentre i pannelli b) e d) riportano le misure del sistema EC1.

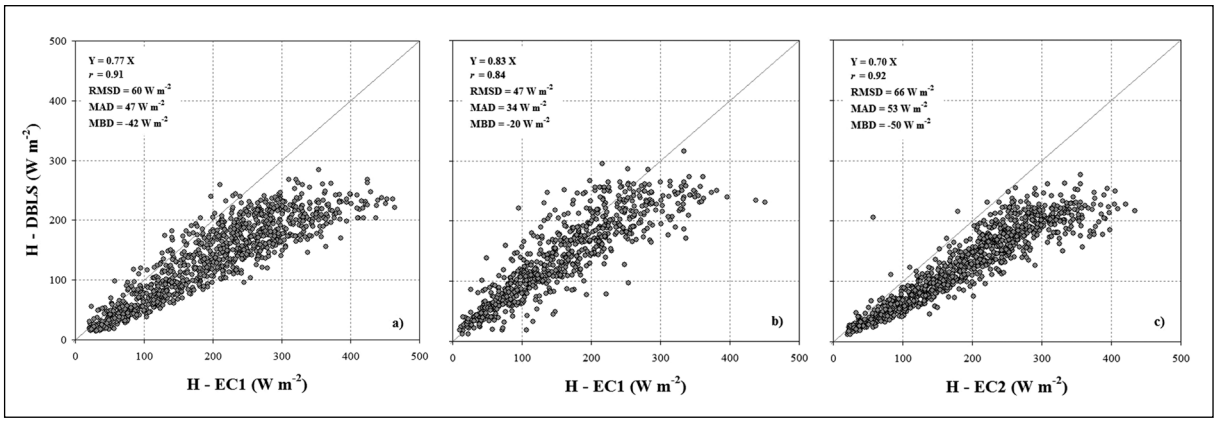

Fig. 3 - Scatterplots of the sensible heat flux measurements collected using the EC and DBLS methods during: a) 2007, b) 2008 and c) 2009. The fluxes from the DBLS were retrieved by means of the standard approach (SBL-MOST).
Fig. 3 - Diagrammi a dispersione del flusso di calore sensibile misurato dai sistemi EC e DBLS durante: a) 2007, b) 2008 e c) 2009. I flussi del DBLS sono stati ricavati mediate il metodo standard (SBL-MOST).

(Fig. 2c). In contrast, *H* measured via EC (Fig. 2d) shows only a feeble response to shadowing; this is, at least in part, due to the erratic nature of the EC measurements of *H*.

The noisy nature of the measurements of *H* collected by EC1 may be partially attributed to the smaller footprint of the EC system compared to that of the DBLS. The smaller footprint implies that the EC measurements are more sensitive to crop cover heterogeneity than the DBLS. The smaller footprint also suggests that the source area of the EC system is more variable over time. Conversely, the larger footprint of DBLS has a smoothing effect on the observations by reducing the variability in the vegetation fraction within the source area.

There are also significant discrepancies between the flux measurements from the two techniques with the values observed by EC1 tending to exceed those from DBLS (Fig. 3). These differences are particularly pronounced during midday when the magnitude of *H* is greater. The largest underestimates of *H* by DBLS occurred in 2007 and 2009 with MBD of –42 and –50 W m^{-2}, respectively; similarly, the slope of the best-fit line forced through the origin were equal to 0.77 and 0.70 for 2007 and 2009, respectively, whereas the *r* values were 0.91 and 0.92. For the measurements collected during 2008, MBD, slope and *r* were -20 W m^{-2}, 0.83, and 0.84, respectively. As can be seen in Fig. 3, the greater agreement between measurements of *H* collected during 2008 is also corroborated by the lower RMSD and MAD compared to 2007 and 2009. On the other hand, it can be noticed that the correlation between the measurements increases with the increasing size and overlap of the EC and DBLS footprints.

In order to quantify the effects of the underestimation of *H* by DBLS on a seasonal timescale, mean values were calculated for each half-hourly period during the day using all the data collected in a given year (Fig. 4). These plots reaffirm that DBLS underestimated *H* compared

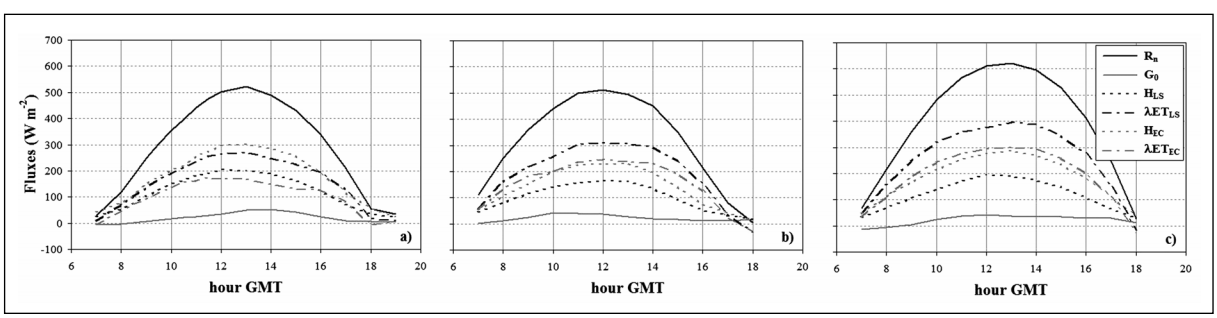

Fig. 4 - Seasonal averages of the half-hour measurements of net radiation, soil, sensible, and latent heat fluxes measured during a) 2007, b) 2008, and c) 2009. The subscript LS identifies the fluxes retrieved by the standard approach stand-alone laser scintillometer approach and the subscript EC refers to the eddy covariance observations.
Fig. 4 - Medie stagionali delle misure semi-orarie di radiazione netta, e flussi di calore sensibile, latente e nel suolo durante il a) 2007, b) 2008, c) 2009. Il pedice LS identifica i flussi ricavati dallo scintillometro laser con metodo standard mentre il pedice EC si riferisce alle misure con sistema di correlazione turbolenta.

to EC and show that the maximum difference occurs during midday. In 2007 and 2009 the discrepancy during peak hours was about 100 W m^{-2}, which corresponds to 22% and 18% of the available energy, respectively, during each year. In 2008 the discrepancy was about 70 W m^{-2} or 15% of the available energy.

4.2 Diagnosis of Friction Velocity for Tall Sparse Canopies

Equation (9) highlights the direct proportionality between H and both u_* and T_* estimates (Eqs. 8a and 8b) for DBLS. Additionally, the dependence of both u_* and T_* to L (through the universal functions f_ε and f_T) causes an interdependence between the accuracy of the two estimates. The analysis of u_* data reported in Fig. 5 indicates that the major source of error in DBLS H is linked to u_*. The plots in Fig. 5 clearly show significantly lower values retrieved by DBLS compared to those from EC for all the three years. Although the values of u_* were well-correlated for 2007 (r = 0.80), the slope of the best-fit line (slope = 0.40) considerably differs from unity and the intercept (intercept = 0.08) is not negligible; MBD (-0.25 m s^{-1}) also suggests DBLS systematically underestimates u_*. The data from 2009 showed similar results. Furthermore, data from 2008 showed more scatter (r = 0.55), although a smaller systematic underestimation (MBD = -0.07 m s^{-1}) is observed by comparison with the other two years.

While previous studies (*e.g.*, de Bruin *et al.*, 2002; Hartogensis *et al.*, 2002) have shown that DBLS tends to underestimation u_* compared to EC, the differences are more evident in this study. Additionally, the results of this study indicate that the underestimation of u_* is greater when both the DBLS and EC data are collected close to the surface (*i.e.*, 2007 and 2009). This behavior can be understood by analyzing the depth of the RL at the study site. A comparison of the measurement heights of both the DBLS and EC systems to z^* calculated using a variety of methods (Cellier and Brunet, 1992; Garratt, 1978, 1980; Graefe, 2004; Verhoef *et al.*, 1997) indicates that measurements were collected within the RL. Thus, MOST, as well as the universal functions based on it, are likely invalid.

In order to test the applicability of MOST, Foken and Wichura (1996) suggested comparing the ratio of standard deviation of the vertical wind speed (σ_w) to u_* obtained by EC with that computed using the experimentally-derived function developed by Panofsky *et al.* (1977) based on MOST. More specifically, the relationship as expressed by Panofsky and Dutton (1984):

$$\frac{\sigma_w}{u_*} = 1.3\left(1 + 2.5\frac{z - d_0}{L}\right)^{1/3} \qquad (19)$$

was used. The observed ratio was consistently lower than the ratio predicted by MOST (Fig. 6) with a bias of 0.20. The value of 1.1, observed in near-neutral condition, agrees with those obtained just above canopy surface by Raupach *et al.* (1996); these authors suggested that low values are indicative of the organized turbulent structures typical of the RL.

In order to circumvent the potentially adverse effects of collecting measurements in the RL, estimates of u_* obtained from Eq. (12) using direct measurements of U recorded by the cup anemometers (one for each EC installation) were evaluated. Focusing on the daytime period to ensure sufficiently high wind speeds, u_* was calculated via Eq. (12) assuming that d_0 and z_{0m} were 2/3 and 1/9 the canopy height, respectively.

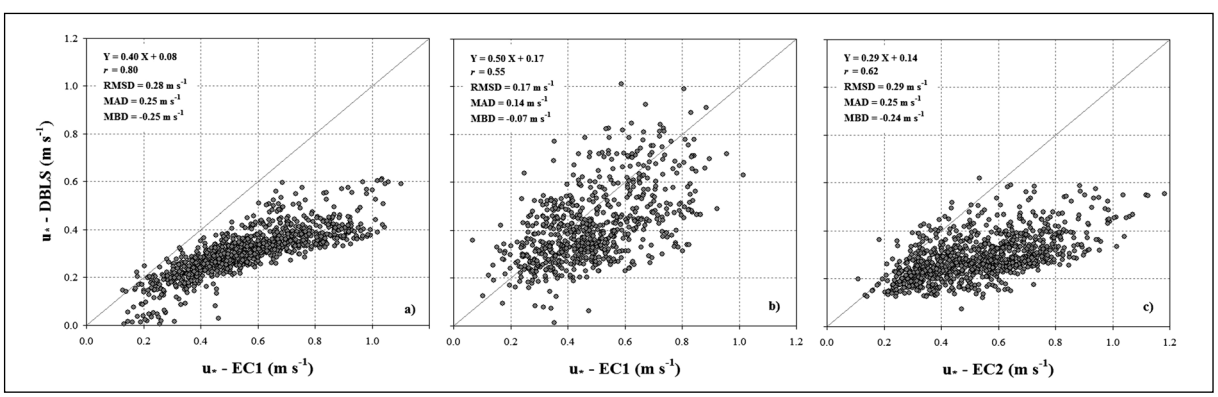

Fig. 5 - Scatterplots comparing the friction velocity retrieved from EC and DBLS during a) 2007, b) 2008 and c) 2009 are shown.

Fig. 5 - Diagrammi a dispersione delle velocità d'attrito ricavate dai sistemi EC e DBLS durante il a) 2007, b) 2008 e c) 2009.

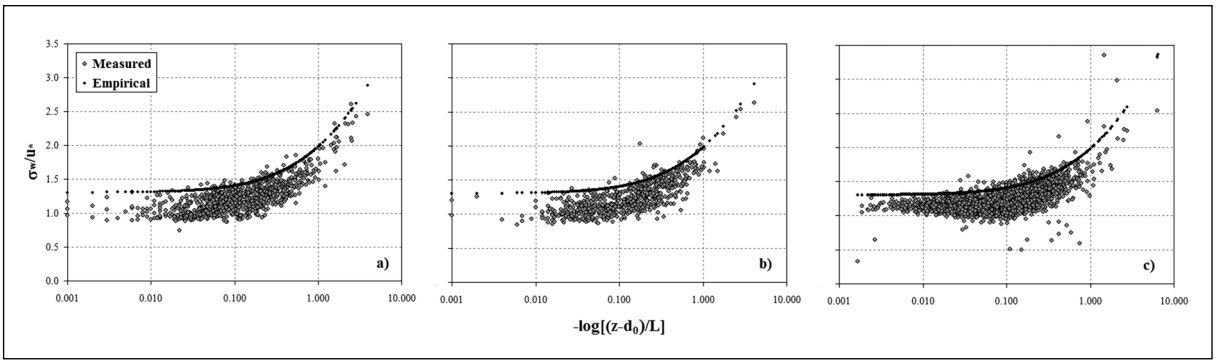

Fig. 6 - Comparison of the ratio of the standard deviation of vertical wind velocity and friction velocity (σ_w/u_*) obtained from EC1 and the empirically-derived relationship of Panofsky and Dutton (1984) for a) 2007, b) 2008, and c) 2009.
Fig. 6 - Confronto tra i valori misurati dal sistema EC1 e i valori ricavati con la relazione empirica di Panofsky and Dutton (1984) del rapporto tra la deviazione standard della componente verticale della velocità del vento e la velocità d'attrito (σ_w/u_*) per gli anni a) 2007, b) 2008 e c) 2009.

Notwithstanding the simple parameterization of d_0 and z_{0m}, the agreement between the values of u_* calculated from Eq. (12) and those obtained from EC was quite good for all three years (Fig. 7). The near-zero MBD values (equaled 0.01 m s^{-1}, 0.02 m s^{-1}, and 0.02 m s^{-1} for 2007, 2008 and 2009, respectively) suggest that the assumed roughness parameters provide an almost unbiased fitting of the observed u_* values; this finding was further corroborated by a sensitivity analysis performed on Eq. (12). This sensitivity analysis was conducted by calculating u_* via Eq. (12) using a sampling of the plausible values of d_0 and z_{0m} and comparing the results with the EC observations. The results of the sensitivity analysis, which are summarized in Tab. 1, demonstrate that the best estimates of u_* were obtained using the adopted parameterization. Parameterizing d_0 as 2/3 the canopy height and z_{0m} as 1/9 the canopy height not only yielded a best-fit line with a slope near one, it also yielded the lowest relative error (RE). It is also interesting to note that the errors reported in Tab. 1 are consistently less than those obtained using the standard estimation technique based on MOST; this seems to suggest that the alternative technique can provide better estimates of u_* using Eq. (12) even when d_0 and z_{0m} are poorly defined.

4.3 Analysis of the Proposed Alternative Approach

On the basis of the findings reported in the previous section, the turbulent fluxes obtained with the alternative methodology were analyzed for the three study periods. The scatterplots in Fig. 8 report the

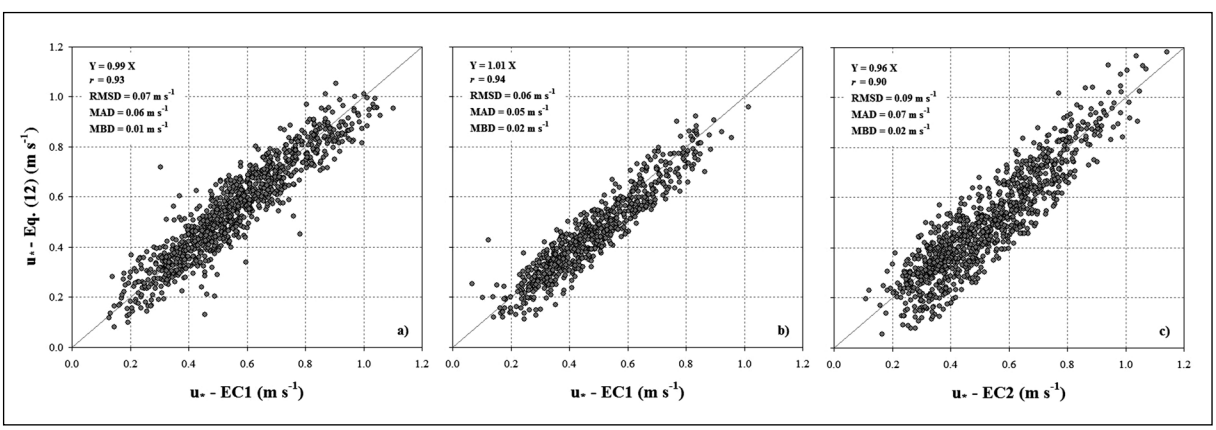

Fig. 7 - Scatterplots comparing the friction velocity measured by the EC systems and derived from the cup anemometer data from a) 2007, b) 2008 and c) 2009 using Eq. (12). The zero-plane displacement height and roughness length for momentum are parameterized as 2/3 and 1/9 of the canopy height, respectively.
Fig. 7 - Diagrammi a dispersione confrontanti la velocità d'attrito misurata dal sistemi EC e ricavati mediante l'Eq. (12) dalle misure degli anemometri a coppe acquisite durante il a) 2007, b) 2008 e c) 2009. L'altezza di traslazione del piano zero e la lunghezza d'attrito per la quantità di moto sono stati assunti rispettivamente pari a 2/3 ed 1/9 dell'altezza della vegetazione.

Parameters	2007		2008		2009	
	RE	slope	RE	slope	RE	slope
$d_0 = 2/3\ h_c$ $z_{0m} = 1/10\ h_c$	12.0	1.02	12.8	1.04	21.6	1.11
$d_0 = 1/4\ h_c$ $z_{0m} = 1/10\ h_c$	15.4	1.10	16.4	1.11	29.7	1.22
$d_0 = 2/3\ h_c$ $z_{0m} = 1/8\ h_c$	12.6	0.93	12.0	0.96	17.3	1.03
$d_0 = 2/3\ h_c$ $z_{0m} = 1/9\ h_c$	11.7	0.99	11.9	1.00	18.1	1.05
$d_0 = 2/3\ h_c$ $z_{0m} = 1/7\ h_c$	15.3	0.88	13.6	0.90	17.8	0.95

Tab. 1 - Sensitivity analysis of u_* derived from Eq. (12) to the parameterization of surface roughness. Statistics were derived by comparing the modeled values with the EC measurements at 30-min time scale. Slope values were obtained by forcing the regression line through the origin.
Tab. 1 - Analisi di sensitività della u_* ricavata dall'Eq. (12) alla parametrizzazione della rugosità di superficie. Gli indici statistici sono stati ricavati confrontando i valori modellati con le misure EC alla scala temporale di 30-min. I valori di pendenza sono stati ottenuti forzando la regressione lineare per l'origine.

comparison between *H* measured by EC and those derived from DBLS observations using the alternative approach, highlighting the improved agreement in the measurement of *H* for all three years; the slopes of the regression line (forced through the origin) were very close to one. In addition, the lower RMSD and MAD, approximately 40 W m^{-2} and 30 W m^{-2}, respectively, compared to those obtained using the standard approach, which were *circa* 60 W m^{-2} and 45 W m^{-2}, respectively, indicate that these estimates of *H* are more accurate than those determined using the standard approach. Additionally, these values of MAD and RMSD are comparable to those found by other authors (Ezzahar *et al.*, 2009; Savage, 2008; Odhiambo and Savage, 2009b; Alfieri *et al.*, 2011) who analyzed the measurement uncertainty associated with the two measurement techniques. The MBD between the measurements of *H* was -12 W m^{-2}, -2 W m^{-2}, and -3 W m^{-2}, respectively, for 2007, 2008, and 2009. Nonetheless, there is still significant scatter between EC2 and DBLS measurements. This is due, in part, to the differences in footprint and, in part, to the sparse

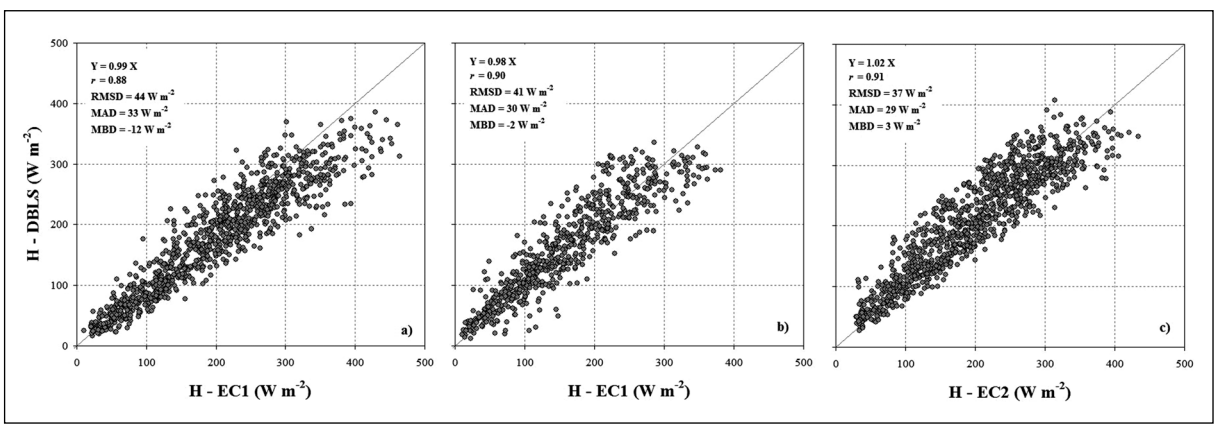

Fig. 8 - Scatterplots comparing the EC and DBLS sensible heat fluxes measured during: a) 2007, b) 2008 and c) 2009. The DBLS fluxes were retrieved by means of the proposed alternative approach.
Fig. 8 - *Diagrammi a dispersione confrontanti i flussi di calore sensibile ricavati dai sistemi DBLS e EC durante: a) 2007, b) 2008 e c) 2009. I flussi DBLS sono stati ottenuti mediate l'approccio alternativo proposto.*

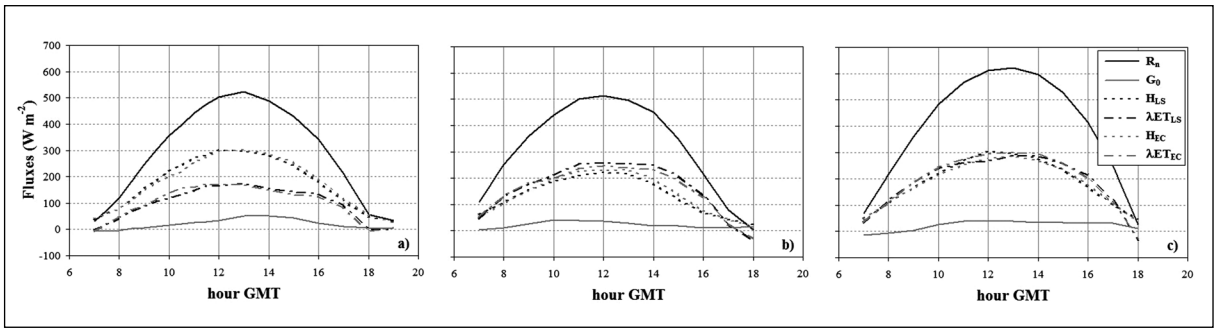

Fig. 9 - Seasonal averages of the half-hour measurements of net radiation, soil, sensible, and latent heat fluxes measured during a) 2007, b) 2008, and c) 2009. The subscript LS identifies the fluxes retrieved by the proposed alternative approach and the subscript EC refers to the eddy covariance observations.
Fig. 9 - Medie stagionali delle misure semi-orarie di radiazione netta, e flussi di calore sensibile, latente e nel suolo durante il a) 2007, b) 2008, c) 2009. Il pedice LS identifica i flussi ricavati dallo scintillometro laser mediante l'approccio alternativo proposto mentre il pedice EC si riferisce alle misure con sistema di correlazione turbolenta.

canopy structure of the olive orchard. The season-average fluxes computed for H calculated using the alternative methodology are shown in Fig. 9; these plots are analogous to Fig. 4. The graphs reaffirm that the systematic biases between the fluxes retrieved by the two methodologies have been largely eliminated.
The scatterplot of the total daytime evapotranspiration (mm d^{-1}, ET_d) obtained by the integration of daytime λET estimated using the EC and DBLS techniques, respectively, is shown in Fig. 10. More specifically, ET_d values from EC are compared with those derived from both SBL-MOST and the alternative methodology. The scatterplot clearly highlights the overestimation of ET_d by the standard approach with a resulting bias of about 1 mm d^{-1}. For all years, the ET_d retrieved using SBL-MOST had an average RMSD, MAD, and RE of 1.14 mm d^{-1}, 1.04 mm d^{-1}, and 47.2%, respectively (Tab. 2). On the other hand, the alternative approach returns estimates in better agreement with the EC measurements with an average RMSD, MAD, and RE equal to 0.43 mm d^{-1}, 0.35 mm d^{-1}, and 16%, respectively. These results are consistent with those reported for similar studies conducted over other land cover types (Shuttleworth, 2008; Wilson *et al.*, 2001), as well as the findings discussed in a recent review article by Allen *et al.* (2011) indicating measurement errors of 10-15% are typical for both EC and scintillometry. Additionally, the values obtained from both EC and ALT methods are better in line with the expected values for this crop during the growing season under water deficit conditions.

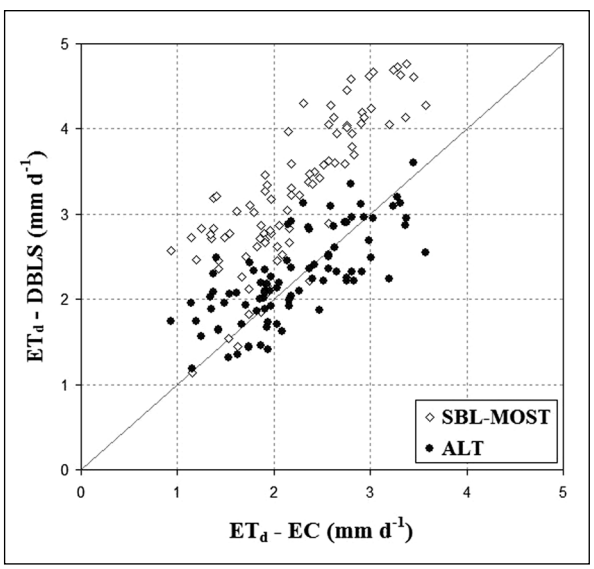

Fig. 10 - Scatterplot comparing daily evapotranspiration measured by EC and those retrieved from the scintillometer measurements by means of the standard approach (SBL-MOST) and the alternative approach (ALT).
Fig. 10 - Diagramma a dispersione confrontante le misure di evapotraspirazione giornaliera ottenute dai sistemi EC e dallo scintillometro mediante il metodo standard (SBL-MOST) e quello alternativo proposto (ALT).

5. SUMMARY AND CONCLUSIONS

The applicability of the displaced-beam laser scintillometer (DBLS) for the estimation of surface energy fluxes in sparse olive orchard was analyzed with a particular emphasis on the computation of turbulent fluxes (H and λET) under unstable conditions and to its effect on the estimates of daytime actual evapotranspiration, ET_d. In the case of sparse canopies, where the spatial variability of the energy fluxes can be significant, the use of scintillometry overcomes the limits of other common micrometeorological instruments (e.g., eddy covariance, surface

Dataset	$\overline{ET_d}$	SBL-MOST			Alternative approach		
		MAD	RMSD	RE	MAD	RMSD	RE
	(mm d^{-1})	(mm d^{-1})		(%)	(mm d^{-1})		(%)
2007	1.75	1.04	1.12	59.1	0.36	0.44	20.5
2008	2.04	0.71	0.91	34.8	0.30	0.38	14.9
2009	2.88	1.27	1.31	44.0	0.37	0.46	12.8
All	2.20	1.04	1.14	47.2	0.35	0.43	15.9

$$\overline{ET_d} = \frac{1}{N}\sum_{i=1}^{N} M_i \qquad RMSD = \sqrt{\left(\frac{1}{N}\sum_{i=1}^{N}(M_i - O_i)^2\right)} \qquad MAD = \frac{1}{N}\left(\sum_{i=1}^{N}|M_i - O_i|\right) \qquad RE = \frac{MAD}{\overline{ET_d}} \times 100$$

N is the number of daily observations, M_i is the value of the i-th EC flux, O_i is the value of the i-th DBLS flux.

Tab. 2 - Statistics derived by the comparison of DBLS (MOST and Alternative methods) and EC daily evapotranspiration for the three years and over the full dataset.
Tab. 2 - Indici statistici derivati dal confronto dell'evapotraspirazione giornaliera da DBLS (metodi MOST e Alternative) e EC sull'intero set di dati e nei tre anni separatamente.

renewal and Bowen ratio) related to the relatively small size of the source area. Field scale average representative values can be obtained using a single installation, rather than multiple instruments, which makes scintillometry a better reference for model validation. This study demonstrates that scintillometry allows an easy detection of changing field-average environmental conditions on both clear-sky and cloudy days, which is a desirable feature of a reference dataset when it is used for instance for the validation of models applied at a specific time of the day (i.e., thermal remote sensing based). Nonetheless, scintillometry is susceptible to errors in the estimations of λET because the water vapor flux is determined as the residual of the surface energy balance, which can be a significant issue in hydrological applications; this is a common limit for several other techniques, and only eddy covariance represents a notable exception.

Data collection, carried out in an olive orchard located in southern Italy (Sicily) using a DBLS and two eddy covariance systems (EC1 and EC2), allowed a preliminary comparison of H measured by the DBLS and EC systems, that showed how DBLS tended to underestimate the fluxes of about 23%, particularly during mid-day. The underestimate of H causes a similar overestimation of λET because it is determined as residual of the energy balance with the DBLS technique. The bias between the two measurements was explained by the underestimation of u_* using the standard SBL-MOST approach. In turn, the underestimate of u_* compared to the measurements from the EC systems, as well as the expected value based on the relationship of Panofsky *et al.* (1977), is likely due to a failure of MOST to accurately describe the turbulent conditions within the RL.

The comparison between u_* measured by EC systems and the values obtained by the application of the commonly-used logarithmic profile shows a close agreement. This suggests that the latter estimates of u_* should be used as support to retrieve H from DBLS. Moreover, the good agreement between the u_* values from the EC systems and those derived from Eq. (15) indicates that d_0 and z_{0m}, which are difficult to define for sparse tall crops, can be reasonably modeled using the "classical" approach based on the fraction of canopy height approach. The proposed alternative approach takes advantage of this finding to determine H from DBLS by using these u_* estimates and T_* values derived from the equation proposed by de Bruin *et al.* (1993).

The comparison of the results obtained from the proposed approach with the EC measurements shows a significant improvement in the agreement of the two datasets, with a linear regression slope (forced through the origin) for H close to unity and

MBD very close to zero. Using this method, RMSD averaged about 40 W m^{-2} while MAD was, on average, approximately 30 W m^{-2}; correspondingly, the average error in ET_d is about 0.4 mm d^{-1} or, equivalently, 16%. These results are consistent with the findings of other studies (Allen *et al.*, 2011; Shuttleworth, 2008; Wilson *et al*, 2001) performed in comparable experimental setups.

The proposed solution implies the need of additional standard low-frequency wind speed measurements, which can be collected without increasing significantly neither the installation cost nor the complexity. The use of a standard wind speed profile allows avoiding site-specific empirical correction coefficients, which use was often suggested in the literature for other micro-meteorological approaches (Bowen ratio, surface renewal).

Similar studies on sparse vegetation performed using the surface renewal method (Mengistu and Savage, 2010) also highlighted the need of different formulation for the inertial and roughness sub-layers; in particular, Castelví (2004) successfully combined surface renewal and similarity theory to estimate *H* in both sub-layers avoiding the need of calibration. However, these formulations also require additional wind speed measurements above canopy to quantify the effects of stability parameter during unstable conditions.

These alternatives to the common EC technique have highlighted both the issues related to roughness sub-layer as well as the general need of auxiliary measurements (i.e., wind speed) to correctly quantify surface fluxes; our proposed alternative approach is in line with these findings and is based on the use of similar additional measurements. Studies on surface renewal techniques have already demonstrated their applicability over different conditions using analogous inputs dataset (Castelví *et al.*, 2006); the results obtained during this experiment, even if it represent a fist application of the proposed methodology, seem encouraging for further tests and validations over areas characterized by different crop types.

ACKNOWLEDGEMENTS

The authors thank the *Ente per le Nuove Tecnologie, l'Energia e l'Ambiente* (ENEA) of Palermo, with in particular F. Monteleone and F. Anello, for the helpful collaboration in the scintillometer data acquisition, instrument installation and management, the SIAS (*Servizio Informativo Agrometeorologico Siciliano*) of the *Assessorato Agricoltura e Foreste della Regione Siciliana* for supporting both the scintillometer and the eddy covariance installations, and the "*Azienda Agricola Rocchetta di Angela Consiglio*" for kindly hosting the experiment. This work has been partially funded by the AGROCLIMA-SICILIA project of the *Assessorato Agricoltura e Foreste della Regione Siciliana* and by PRIN2007-Agnese, co-funded by *Università degli Studi di Palermo* and MIUR.

REFERENCES

Alfieri J.G., Kustas W.P., Prueger J.H., Hipps L.E., Chavez J.L., French A.N., Evett S.R., 2011. Intercomparison of nine micrometeorological stations during the BEAREX08 field campaign. J. Atmos. Ocean. Tech., 28: 1390-1406.

Allen R.G., Pereira L.S., Howell T.A., Jensen M.E., 2011. Evapotranspiration information reporting: I. Factors governing measurement accuracy. Agric. Water Mange. 98: 899-920.

Aubinet M., Grelle A., Ibrom A., Rannik U., Moncrieff J., Foken T., Kowalski A.S., Martin P.H., Berbigier P., Bernhofer C., Clement R., Elbers J., Granier A., Grunwald T., Morgenstern K., Pilegaard K., Rebmann C., Snijders W., Valentini R., Vesala T., 2000. Estimates of the annual net carbon and water exchange of forests: The EUROFLUX methodology. Adv. Ecol. Res. 30: 113-175.

Brutsaert W.H., 1982. Evaporation into the Atmosphere. Theory, History and Applications. Kluwer Academic Publishers, 308 pp.

Cammalleri C., Anderson M.C., Ciraolo G., D'Urso G., Kustas W.P., La Loggia G., Minacapilli M., 2012. Applications of a remote sensing-based two-source energy balance algorithm for mapping surface fluxes without in situ air temperature observations. Remote Sens. Environ. 124: 502-515.

Castelví, F., 2004. Combining surface renewal analysis and similarity theory: a new approach for estimating sensible heat flux. Water Resour. Res. 40, W05201, 1-20.

Castelví F., Snyder,R.L., Baldocchi D.D., Martínez-Cob A., 2006. A comparison of new and existing equations for estimating sensible heat flux using surface renewal and similarity concepts. Water Resour. Res. 42, W08406, 1-18.

Cellier P., Brunet Y., 1992. Flux-gradient relationship above tall plant canopies. Agric. For. Meteorol. 58: 93-117.

Chen W., Novak M.D., Black T.A., 1997. Coherent eddies and temperature structure functions for

three contrasting surfaces. Part II: renewal model for sensible heat flux. Boundary Layer Meteorol. 84: 125-147.

Choi M., Kustas W.P., Anderson M.C., Allen R.G., Li F., Kjaersgaard J.H., 2009. An intercomparison of three remote sensing-based surface energy balance algorithms over a corn and soybean production region (Iowa, U.S.) during SMACEX. Agric. For. Meteorol. 149(12): 2082-2097.

de Bruin H.A.R., Kohsiek W., van den Hurk B.J.J.M., 1993. A verification of some methods to determine the fluxes of momentum, sensible heat, and water vapour using standard deviation and structure parameter of scalar meteorological quantities. Boundary Layer Meteorol. 63: 231-257.

de Bruin H.A.R., Meijninger W.M.L., Smedman A.-S., Magnusson M., 2002. Displaced-beam small aperture scintillometer test. Part I: The Wintex data-set. Boundary Layer Meteorol. 105: 129-148.

de Ridder K., 2010. Bulk transfer relations for the roughness sublayer. Boundary Layer Meteorol. 134: 257-267.

Ezzahar J., Chehbouni A., Hoedjes J., Ramier D., Boulain N., Boubkraoui S., Cappelaere B., Descroix L., Mougenot B., Timouk F., 2009. Combining scintillometer measurements and an aggregation scheme to estimate area-averaged latent heat flux during the AMMA experiment. J. Hydrol. 375: 217-226.

Falge E., *et al.*, 2001. Gap filling strategies for long term energy flux data sets. Agric. For. Meteorol. 107: 71-77.

Foken T., Wichura B., 1996. Tools for the quality assessment of surface-based flux measurements. Agric. For. Meteorol. 78: 83-105.

French A.N., Jacobs F., Anderson M.C., Kustas W.P., Timmermans W., Gieske A., Su Z., Su H., McCabe M.F., Li F., Prueger J.H., Brunsell N., 2005. Surface energy fluxes with the Advanced Spaceborne Thermal Emission and Reflection radiometer (ASTER) at the Iowa 2002 SMACEX site (USA). Remote Sens. Environ. 99: 55-65.

Garratt J.R., 1978. Flux profile relations above tall vegetation. Q. J. Roy. Meteorol. Soc. 104: 199-211.

Garratt J.R., 1980. Surface influence upon vertical profiles in the atmospheric near-surface layer. Q. J. Roy. Meteorol. Soc. 106: 803-819.

Göckede M., Markkanen T., Mauder M., Arnold K., Leps J., Foken T., 2005. Validation of footprint models using natural tracer measurements from a field experiment. Agric. For. Meteorol. 135: 314-325.

Graefe J., 2004. Roughness layer corrections with emphasis on SVAT model applications. Agric. For. Meteorol. 124: 237-251.

Hartogensis O.K., 2006. Exploring scintillometry in the stable atmospheric surface layer. PhD Thesis, Wageningen University, Wageningen, The Netherlands, 240 pp.

Hartogensis O.K., de Bruin H.A.R., van de Wiel B.J.H., 2002. Displaced-beam small aperture scintillometer test. Part II: Cases-99 stable boundary-layer experiment. Boundary Layer Meteorol. 105: 149-176.

Hill R.J., 1997. Algorithms for obtaining atmospheric surface-layer fluxes from scintillation Measurements. J. Atmos. Ocean. Tech. 14: 456-467.

Hill R.J., Clifford S.F., 1978. Modified spectrum of atmospheric turbulence fluctuations and its application to optical propagation. J. Opt. Soc. Am. 68: 892-899.

Hoedjes J.C.B., Chehbouni A., Ezzahar J., Escadafal R., de Bruin H.A.R., 2007. Comparison of large aperture scintillometer and eddy covariance measurements: can thermal infrared data be used to capture footprint-induced differences? J. Hydrometeorol. 8: 144-159.

Kaimal J.C., Finnigan J.J., 1994. Atmospheric Boundary Layer Flows. Oxford University Press, New York, USA, 289 pp.

Kormann R., Meixner F.X., 2000. An analytical footprint model for non-neutral stratification. Boundary Layer Meteorol. 99: 207-224.

Manca G., 2003. Analisi dei flussi di carbonio di una cronosequenza di cerro (Quercus Cerris L.) dell'Italia centrale attraverso la tecnica della correlazione turbolenta. PhD Thesis, Università degli Studi della Tuscia, Viterbo, Italy, 229 pp.

Mengistu M.G., Savage M.J., 2010. Surface renewal method for estimating sensible heat flux. Water SA 36(1), 9-18.

Moene A.F., 2003. Effects of water vapour on the structure parameter of the refractive index for near-infrared radiation. Boundary Layer Meteorol. 107: 635-653.

Mölder M., Grelle A., Lindroth A., Halldin S., 1999. Flux-profile relationships over a boreal forest-roughness sublayer corrections. Agric. For. Meteorol. 98-99: 645-658.

Moncrieff J.B., Massheder J.M., de Bruin H.A.R., Elbers T., Friborg J., Heusinkveld B., Kabat P., Scott S., Soegaard H., Verhoef A., 1997. A

system to measure surface fluxes of momentum, sensible heat, water vapour and carbon dioxide. J. Hydrol. 188-189: 589-611.
Odhiambo G.O., Savage M.J., 2009a. Surface layer scintillometry for estimating the sensible heat flux component of the surface energy balance. S. Afr. J. Sci. 105(5-6): 208-216.
Odhiambo G.O., Savage M.J., 2009b. Sensible heat flux by surface layer scintillometry and eddy covariance over mixed grassland community as affected by Bowen ratio and MOST formulations for unstable conditions. J. Hydrometeorol. 10(2): 479-492.
Panofsky H.A., Dutton J.A., 1984. Atmospheric Turbulence. Wiley, New York, USA, 397 pp.
Panofsky H.A., Tennekes H., Lenshow D.H., Wyngaard J.C., 1977. The characteristics of turbulent velocity components in the surface layer under convective conditions. Boundary Layer Meteorol. 11: 355-361.
Papale D., 2006. Il progetto CarboItaly: una rete nazionale per la misura di sink forestali e agricoli italiani e lo sviluppo di un sistema di previsione dell'assorbimento dei gas serra. Forest@ 3(2): 165-167.
Paulson C.A., 1970. The mathematical representation of wind speed and temperature pr ofiles in the unstable atmospheric surface layer. Appl. Meteorol. 9: 857-861.
Pernice F., Motisi A., Rossi F., Georgiadis T., Nardino M., Fontana G., Dimino G., Drago A., 2009. Micrometeorological and sap flow measurement of water vapour exchanges in olive: scaling up from canopy to orchard. Acta Hort. 846: 159-166.
Prueger J.H., Hatfield J.L., Kustas W.P., Hipps L.E., MacPherson J.I., Parkin T.B., 2005. Tower and aircraft eddy covariance measurements of water vapor, energy and carbon dioxide fluxes during SMACEX. J. Hydrometeorol. 6: 954-960.
Raupach M.R., Antonia R.A., Rajagopalan S., 1991. Rough-wall turbulent boundary layers. Appl. Mech. Rev. 44: 1-25.
Raupach M.R., Finnigan J.J., Brunet Y., 1996. Coherent eddies and turbulence in vegetation canopies: the mixing-layer analogy. Boundary Layer Meteorol. 78: 351-386.
Rosenberg N.J., Blad B.L., Verma S.B., 1983. Microclimate. The Biological Environment. Wiley, New York, USA, 255-257.
Savage M.J., 2008. Estimation of evaporation using a dual-beam surface layer scintillometer and component energy balance measurements. Agric. For. Meteorol. 149: 501-517.
Schmugge T.J., Kustas W.P., Ritchie J.C., Jackson T.J., Rango A., 2002. Remote sensing in hydrology. Adv. Water Resour. 25: 1367-1385.
Shuttleworth W.J., 2008. Evapotranspiration measurement methods. Southwest Hydrol. 7: 22-23.
Stull R.B., 1988. An Introduction to Boundary Layer Meteorology. Kluwer Academic Publishers, Dordrecht, 666 pp.
Thiermann V., 1992. A displaced-beam scintillometer for line-averaged measurements of surface layer turbulence. Proceedings of the 10th Symposium on Turbulence and Diffusion, 244-247.
Thiermann V., Grassl H., 1992. The measurement of turbulent surface-layer fluxes by use of bichromatic scintillation. Boundary Layer Meteorol. 58: 367–389.
Timmermans W.J., Kustas W.P., Anderson M.C., French A.N., 2007. An intercomparison of the Surface Energy Balance Algorithm for Land (SEBAL) and the Two-Source Energy Balance (TSEB) modelling schemes. Remote Sens. Environ. 108(4): 369-384.
UNEP/MAP-PlanBleu, 2009. State of the Environmental Development in the Mediterranean. Athens, Greece, 204 pp.
Verhoef A., McNaughton K.G., Jacobs A.F.G., 1997. A parameterization of momentum roughness length and displacement height for a wide range of canopy densities. Hydrol. Earth Syst. Sci. 1: 81-91.
Vogt R., Christen A., Pitacco A., 2004. Scintillometer measurements in a cork oak and an olive tree plantation. In: 26th Conference on Agric. For. Meteorol., 23-27 August, Vancouver, BC, Canada.
Webb E.K., 1970. Profile relationships: the log-linear range, and extension to strong stability. Q. J. Roy. Meteorol. Soc. 96: 67-90.
Webb E.K., Pearman G.L., Leuning R., 1980. Correction of flux measurements for density effects due to heat and water vapour transfer. Q. J. Roy. Meteorol. Soc. 106: 85-100.
Wesely M.L., 1976. The combined effect of temperature and humidity fluctuations on refractive index. J. Appl. Meteorol. 15: 43-49.
Wilson K.B., Hanson P.J., Mulholland P.J., Baldocchi D.D., Wullschleger S.D., 2001. A comparison of methods for determining forest evapotranspiration and its components: Sap-flow, soil water budget, eddy covariance and catchment water balance. Agric. For. Meteorol. 106: 153-168.